Crystal habit during crystallization of palm Oil: Effect of time and temperature

[1]Normah, I., [1]Cheow, C.S. and [2]Chong, C.L.

[1]*Department of Food Technology, Faculty of Applied Sciences,*
Universiti Teknologi MARA (UiTM), Shah Alam, 40450 Selangor Darul Ehsan
[2]*Malaysian Palm Oil Board, 43000, Kajang, Selangor Darul Ehsan*

Abstract

Refined bleached and deodorized palm oil (RBDPO) was crystallized from the melt in a thermally controlled water bath at 14 and 22°C for 90 min. Slurries were withdrawn after 5, 15, 30, 60 and 90 min of crystallization for crystal morphology studies. Crystallization was also performed in a similar manner using a Labmax reactor connected to a FBRM detector to obtain the information on crystal count and size distribution during crystallization. Based on the shape of the crystals viewed under the microscope, all crystals appeared as needle shaped spherulitic β´- form at both crystallization temperatures studied. Crystals were slightly larger with increase in crystallization time and at higher crystallization temperature (22°C). Crystals size range between 4.34 to 22.29µm. FBRM recorded high count of crystals with increased in crystallization time and at lower temperature (14°C).

Introduction

The characteristics of crystals formed during the crystallization process especially size and shape are very important as this will influence the separation process which will in turn affect the yield and quality of the resulting fractions. Such characteristics are governed by the crystallization conditions being performed. Rapid crystallization results in the formation of high number of nuclei and thus the formation of numerous crystals with smaller size whereas slow crystallization produced larger crystals which are lesser in number (Campos *et al.*, 2002; Timms, 2005). Several studies on the crystallization of palm oil have been reported previously. van Putte and Bakker (1987) studied on the crystallization kinetics of palm oil where the growth and primary nucleation rates of saturated crystals in palm oil were reported. According to Kawamura (1980), α crystals which appear as dotted spherulites under the microscope are formed when palm oil is crystallized below 24°C while the β´ crystals which appear as dendritic spherulites are formed at temperature above 26°C. The α-form crystals which are very unstable are transformed to other form under isothermal conditions or during heating process and its lifetime is very dependent on the temperature (Kawamura, 1979; Berger, 1989). It has also been shown that different cooling rates also resulted in different morphologies of crystals (Litwinenko, 2001). During crystallization process, agitation is also essential since it allows sufficient mobility of the nuclei to encourage crystal growth. Taylor (1976) observed no change in size or formation of the crystals once the crystals have been fully formed during the time of separation whether agitation are continued or not under the studied cooling conditions and agitation rate. Studies on the count and distribution of RBDPO crystals formed during the crystallization by using Focused Beam Reflectance Measurement (FBRM) have not been reported elsewhere. In this paper, crystallization of RBDPO from the melt was carried out and the effects of crystallization time and temperature on the crystal habit of RBDPO were investigated.

Materials and Methods

Materials

Refined Bleached and Deodorized Palm Oil (RBDPO) with iodine value of 53 was obtained from Golden Jomalina Food Industries Sdn. Bhd (Sijangkang, Selangor Malaysia).

Crystallization process

RBDPO which was placed in a beaker was initially heated in a thermally controlled water bath for 30

*Corresponding author.
Email: *norismel@salam.uitm.edu.my*

min at 70°C to totally melt the oil. The temperature was then reduced to 30°C within one hour followed by reducing to crystallization temperatures of 14 or 22°C within 30 min. Once the oil reached the desired temperatures (14 or 22°C), it was allowed to crystallize until 90 min where the analyses were made at 5, 15, 30, 60 and 90 min to obtain the morphology of the crystals. The beaker content was constantly stirred at 90 rpm through out the process using a stirring motor attached with two blades paddle propeller (Model IKA RW11, Staufen, Germany).

Crystal morphology

Crystal morphology (size and shape) of the RBDPO slurries collected during the crystallization process was obtained using a polarized light microscope (Leica DMLP) equipped with a temperature controlled stage (Linkam TP94 and LNP). Images were recorded using the Leica Qwin V3 imaging system (Cambridge, UK). The temperature of the stage was preset to simulate the crystallization temperatures (14 or 22°C). Zero time denotes the time when the temperature of the water bath reached 14 or 22°C. Samples of slurries were withdrawn at 5, 15, 30, 60 and 90 min of crystallization and placed onto a slide which was then covered with a cover slip. Photographs of the crystals were taken at the magnification of 200x. The lengths of four longest dimensions of each crystal were recorded and an average of at least six crystals was measured during each observation.

Determination of solid fat content (%)

Solid fat content (SFC) was determined according to the PORIM parallel test method (PORIM, 1995) using pulsed nuclear magnetic resonance (pNMR) spectrometry set at 14 and 22°C (Bruker Minispec P20:20 Mhz, Karlsruhe, Germany). RBDPO slurries formed during the crystallization process were withdrawn and filled into the NMR tube up to 3 cm height. The slurries which were withdrawn every 5 min interval during the first half an hour and then every 10 min were immediately measured for the SFC. SFC measurement was done until the end of the day and left overnight before the last measurement was recorded in the following day.

Determination of yield (%) of olein and stearin

Samples were vacuum filtered at the time interval as indicated above through previously weighed buchner funnel, filter paper and side arm flask. The collected oleins and stearins were weighed and yield was calculated as follows:-

$$\text{Yield of olein (\%)} = \frac{\text{weight of olein (g)}}{\text{weight of stearin and olein (g)}} \times 100$$

$$\text{Yield of stearin (\%)} = \frac{\text{weight of stearin (g)}}{\text{weight of stearin and olein (g)}} \times 100$$

Crystal size distribution

Determination of chord length distribution which reflects the crystal size distribution was carried out using the Mettler Toledo Labmax reactor (Schwerzenbach, Switzerland) equipped with Lasentec D600L Focused Beam Reflectance Measurement (FBRM) probe (Lasentec, Richmond, WA, USA). The FBRM records the chord length distribution in terms of the number of counts per second for different crystal size classes. RBDPO (400 ml) was poured into the Labmax reaction vessel consisting of four openings for pouring of sample, insertion of thermometer, FBRM probe and stirrer. RBDPO was initially melted at 70°C for 10 min followed by reducing the temperature to 30°C within 1hr and then further reducing to measuring temperatures (14 or 22°C). Total crystallization time was 90 min. During the run, samples were continuously mixed by a four blade impeller set at 100rpm. Data were collected using 90 log-channel over the range of 1-1000µm with scanning speed set at 2 m/s. Chord length distribution was measured every 15 sec and data were recorded every 5, 15, 30, 60 and 90 min. Count of crystals that fell within the crystal size classes of 1 to 5 µm, 10 to 23 µm, 29 to 86 µm and 100 to 251 µm were recorded.

Statistical analysis

Data were analysed using the Analysis of Variance (ANOVA) to determine significance at 5% level. Duncan Multiple Range Test was used to identify differences between means. The software used was the SAS system for windows release 6.12 SAS Institute Inc. (SAS, 1989).

Results and Discussion

Crystal morphology

Figure 1 and 2 show the crystal photos of RBDPO slurries obtained during the 90 min crystallization at 14°C and 22°C. Crystals were spherulitic in shape at both temperatures and in general were slightly larger with increased in crystallization time. Larger crystals could be due the sufficient time available to enable more molecules to attach to the surface of the existing crystals. Table 1 shows that the crystals produced at 14°C increased significantly ($p<0.05$) with time up to 30 min of crystallization. However, at 22°C, crystals increased significantly ($p<0.05$) with time throughout the 90 min of crystallization. Crystals were larger at 22°C than those observed at 14°C.

At high supercooling temperature (14°C), the
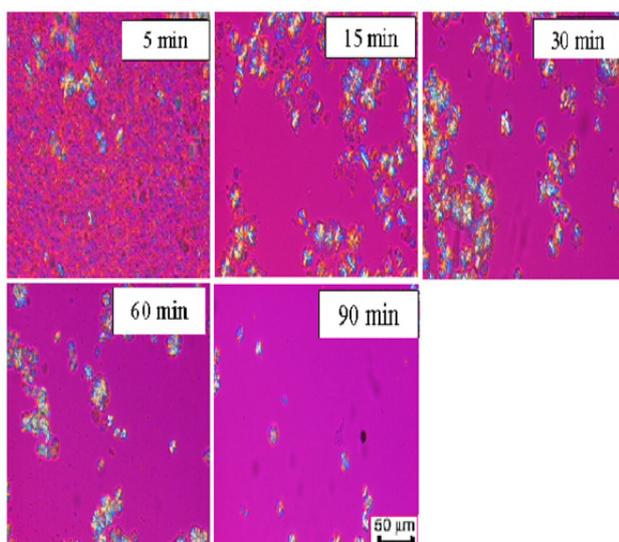
Figure 1. Light microscope photo of crystals formed during 5, 15, 30, 60 and 90 min crystallization of RBDPO at 14°C
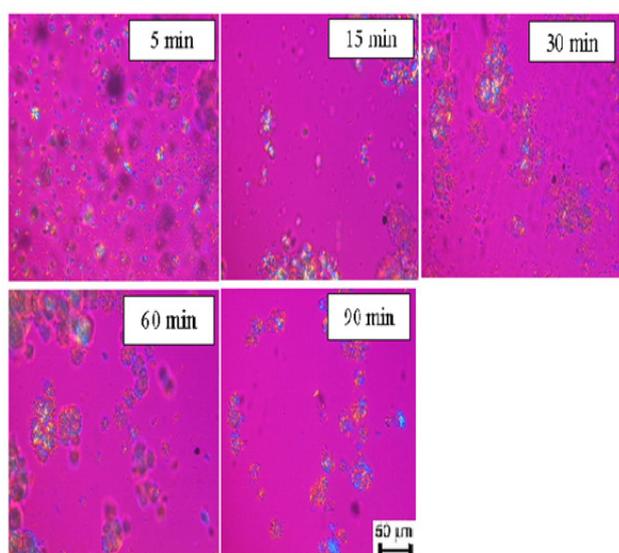
Figure 2. Light microscope photo of crystals formed during 5, 15, 30, 60 and 90 min crystallization of RBDPO at 22°C

Table 1. Crystal size (μm) distribution of RBDPO crystallized at 5, 15, 30, 60 and 90 min at 14 and 22°C as measured by light microscopy

	Crystallization Time (min)				
	5	15	30	60	90
14°C	4.34^{Ad}±0.47	12.04^{Ac}±3.11	17.61^{Ab}±2.30	19.53^{Aab}±3.22	20.72^{Aa}±2.26
22°C	4.78^{Ae}±0.65	12.06^{Ad}±2.49	16.84^{Ac}±0.94	19.98^{Ab}±1.48	22.29^{Aa}±2.89

Values represent means of at least six crystals ± standard deviation.
Means within a row with different lower cases are significantly different (p< 0.05)
Means within a column with different upper cases are significantly different (p< 0.05)

formation of a dense mass of unstable α crystals is enhanced. This resulted in the increase in viscosity. Crystal growth is inversely proportional to the increase in viscosity (Kellens, 1994). The higher the viscosity, the exchange of materials at the surface of crystals is more limited resulting in slower crystal growth (Ibid). Low degree of supercooling tend to produce perfect crystals because the incorporation of molecules on the growing crystal will only take place when the newly formed molecule is exactly in the

right conformation (Timms, 1994). The formation of stable, larger and uniform crystals is desirable to facilitate separation of the oil from the crystals during the filtration process and thus producing higher quality stearin with minimum olein entrainment. Crystal size ranges between 4.34 to 22.29μm (Table 1).

Palm oil appears in four polymorphic forms comprising of the sub α (or β'_2), α, β' (or β'_1) and β (Jacobsberg and Jacqmain, 1976). Fast cooling produces the unstable α crystals which if sufficient energy is provided will be transformed into the β' and β crystals (Ibid). α has little spatial arrangement and a low melting point; β' crystals have a tighter arrangement and higher melting point while β crystals have a dense arrangement and the highest melting point (Bhaskar *et al*., 1998; deMan, 1963). According to Chen *et al*., (2002), isothermal crystallization of refined palm oil below 22°C produced mixed crystals of α and β' polymorphic forms while above 22°C there were only β' crystals. Kawamura (1979), observed dotted spherulites during the isothermal crystallization of palm oil below 24°C whereas above 26°C dendritic spherulites were observed. Based on the shape of the crystals viewed under the microscope in this study, all the crystals are observed to be in the needle shaped spherulitic β'- form at both crystallization temperatures studied. β'-form crystals that produce firm and uniform spherical crystals is desirable in order to obtain good separation compared to the β-form which does not allow easy separation and should be avoided (Kellens, 1994). β'- form also tend to give smooth texture (Berger, 1989).

Crystal size distribution

FBRM is an instrument used to obtain in-line information of particles number and size distribution (Yu *et al*., 2005). It has also been used to estimate crystallization kinetics (Kougoulos *et al*., 2005). The FBRM software includes various weighted distributions which emphasize different size ranges. 1/length weighting emphasizes small particles, square weighting emphasizes larger particles and length weighting exhibits similar behavior to the unweighted counts (Fujiwara *et al*., 2002). In this study, the total count of chord length has been used to indicate the change in crystal number, 1/length weight chord length distribution for the small crystals and the square weight to demonstrate large crystals and crystal growth.

Figure 3 and 4 show the chord length distribution of crystals in the slurry formed during the 90 min crystallization of RBDPO at 14°C. Total count for small crystals was high since at the beginning of crystallization period which is as early as 5 min
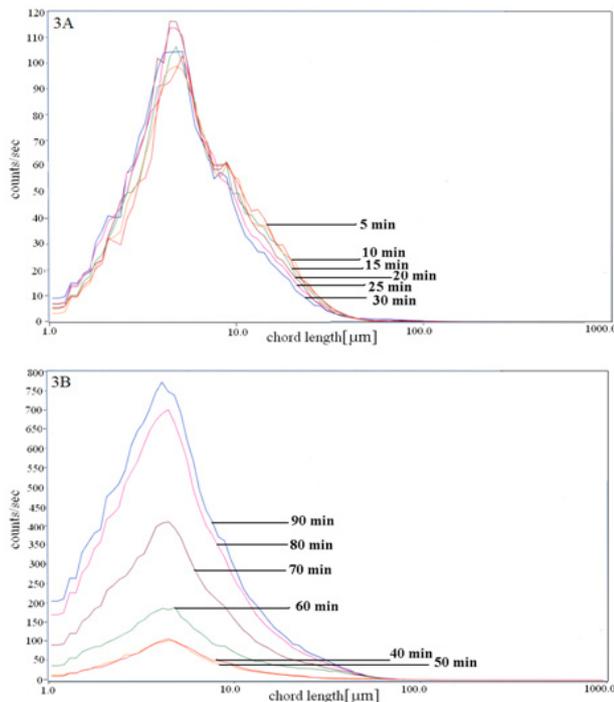
Figure 3. Chord length [μm] distribution of RBDPO crystallized at 14°C for 5 to 30min (A) and 40 to 90 min (B) (1/Lth wt)

Figure 5. Chord length [μm] distribution of RBDPO crystallized at 22°C for 5 to 30min (A) and 40 to 90min (B) (1/Lth wt)

Figure 4. Chord length [μm] distribution of RBDPO crystallized at 14°C for 5 to 30min (A) and 40 to 90min (B) (Sq wt)
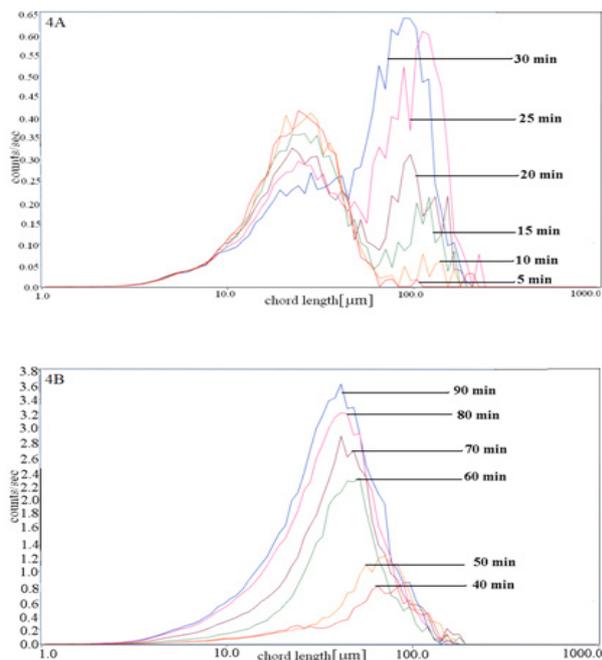
Figure 6. Chord length [μm] distribution of RBDPO crystallized at 22°C for 5 to 30min (A) and 40 to 90min (B) (Sq wt)

crystallization. Throughout the 50 min crystallization, less than 120counts/sec were recorded with peak size range between 5 to 7 μm (Figure 3). The count gradually increased until the end of the 90 min crystallization period reaching 800counts/sec with no further difference in peak size range (Figure 3B). As for large crystals, the count was very low throughout the 90 min crystallization period with less than 3.8counts/sec. (Figure 4). Two peak sizes (50 and 100 μm) were observed during the 30 min

crystallization (Figure 4A). The larger size range could be due to the formation of crystal agglomerates where at high supercooling temperature (14°C), more crystals were formed. As a result, there is a high tendency for the crystals to adhere to each other with time and form agglomerates. Large agglomerates may be formed due to the poor heat transfer and slow agitation (Patience *et al.*, 1999). A considerably slow agitation rate at 90 rpm used in this study may also be the contributing factor to the formation of
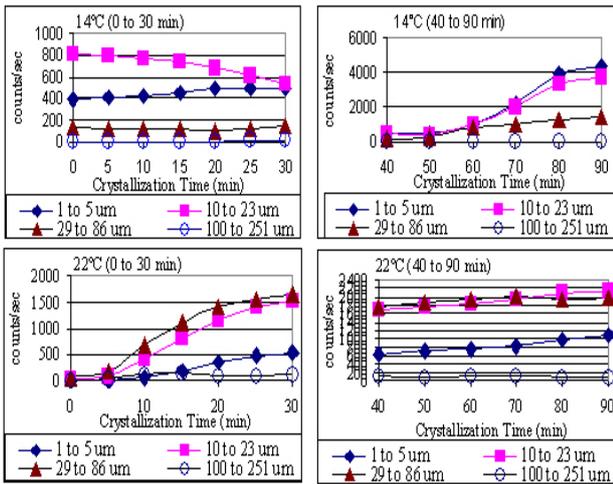
Figure 7. Crystal population [counts/sec] in RBDPO slurries during 0 to 30 min and 40 to 90 min crystallization at 14 and 22°C
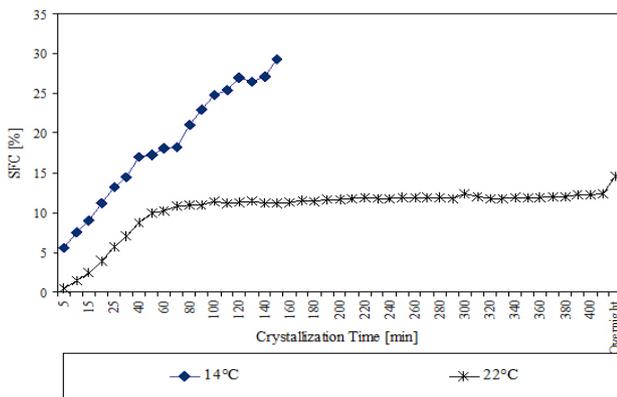
Figure 8. Solid fat content (SFC) [%] of RBDPO crystallized for 90 min at 14 and 22°C
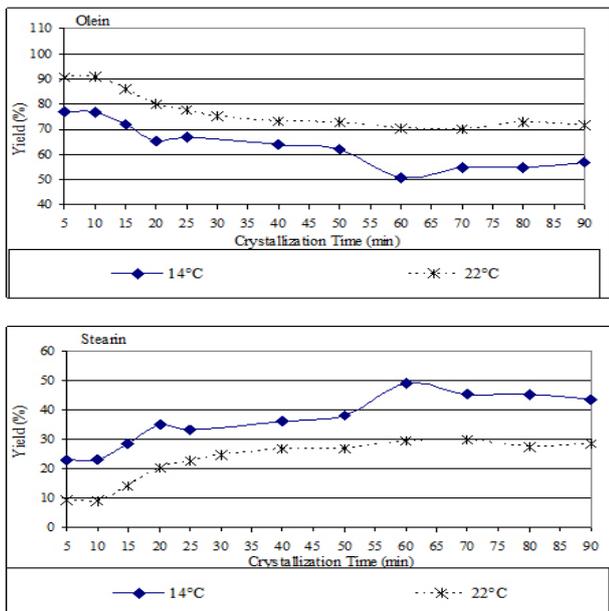
Figure 9. Yield of oleins and stearins during the 90 min crystallization of RBDPO at 14 and 22°C

the agglomerates. Slight shifting to smaller crystal size from 90 to 60 µm throughout the 90 min crystallization was also observed as shown in Figure

4. This probably contributes to the gradual increase in count of small crystals as illustrated in Figure 3B. Shifting of particles size distribution curve to smaller size indicates the possibilities of attrition and breakage of large particles into slightly smaller particles. Breakage leads to increase in number of daughter particles and increase in total number of particles (Zauner and Jones, 2000). However, in this study increased in the total counts suggested the possibility of rapid nucleation taking place and most probably the breakage of crystal agglomerates occurred with time during the isothermal crystallization at the high supercooling temperature. At high degree of supercooling, the addition of molecules at the crystal surface occurs at a faster rate (Timms, 1994). As a result, a new molecule may attach to the neighbouring crystals which are not in a perfect position (Ibid).

At 22°C, the count of small crystals gradually increased with time during the 30 min crystallization with the peak sizes range between 5 to 7 µm and continues to increase but at a slower rate towards the end of 90 min (Figure 5). Slow increase in the count of small crystals is due to the slower nucleation rate occurring at this temperature where some of the crystals nucleated only at the later crystallization period. This finding is in accordance with observation on milk fat crystallization (Herrera and Hartel, 2000). As for large crystals, there was a very slight increased in count between 5 to 10 min crystallization, however, there was no further changes thereafter (Figure 6). The count of large crystal was very low throughout the 90 min crystallization (< 6.5 counts/sec). Peak size was between 90 to 100 µm. This indicated that crystallization at 22°C enhanced crystal growth with the formation of fewer numbers of large crystals. According to Herrera and Hartel (2000) who studied on the nucleation of milk fat, fewer initial crystals were formed at high temperature. Therefore, due to the formation of fewer numbers of initial crystals, crystal growth is enhanced with time.

At 14°C, the count of small crystals was almost twice than those produced at 22°C beginning from 70 min crystallization (Figure 3 and 5). This was probably due to not only rapid nucleation taking place at 14°C, but the prolonged crystallization period with consistent agitation rate enhance heat transfer which subsequently enhance nucleation and collectively increasing the count of small crystals. Slightly higher count of large crystals was observed at 22°C compared to crystallization at 14°C (Figure 4 and 6).

The FBRM data showed that the crystal count gradually increased with time and were higher at lower crystallization temperature (14°C). Although

light microscope data showed that crystal size was slightly larger with increase in crystallization time, there was no indication of size increment from FBRM data. However, both the light microscope and FBRM data showed that crystals were smaller at 14°C where at 14°C, the slurry being dominated by size range of 1 to 23μm compared to 10 to 86μm at 22°C (Figure 7). Thus, crystallization at lower temperature (14°C) produced higher counts and smaller crystals while crystals were slightly larger and gradually increased in count with increased in crystallization time. Due to high supercooling at low temperature (14°C), this enhance the nucleation to occur rapidly whereby crystals were continuously form and increase in number as reflected by the rise in SFC (Figure 8), higher yield of stearins and lower yield of oleins (Figure 9).

Acknowledgements

References

Berger, K.G. 1989. Crystallization behavior of palm oil. Proceedings of the 1989 PORIM International Palm Oil Development Conference 5-9 September 1989, Kuala Lumpur, Malaysia. Module III Chemistry, Technology and Marketing pp. 48-59.

Bhaskar, A.R., Rizvi, S.S.H., Bertoli, C., Fay, L.B. and Hug, B. 1998. A comparison of physical and chemical properties of milk fat fractions obtained by two processing technologies. Journal of the American Oil Chemists' Society 75 (10): 1249 – 1264.

Campos, R., Narine, S.S. and Marangoni, A.G. 2002. Effect of cooling rate on the structure and mechanical properties of milk fat and lard. Food Research International 35: 971-981.

Chen, C.W., Lai, O.M., Ghazali, H.M. and Chong, C.L. 2002. Isothermal crystallization kinetics of refined palm oil. Journal of the American Oil Chemists' Society 79 (4): 403-410.

deMan, J.M. 1963. Polymorphism in milk fat. Dairy Science Abstract 25: 219-221.

Fujiwara, M., Chow, P.S., Ma, D.L. and Braatz, R.D. 2002. Paracetamol crystallization using laser backscattering and ATR-FTIR spectroscopy:metastability, agglomeration and control. Crystal Growth and Design 2(5): 363-370.

Herrera, M.L. and Hartel, R.W. 2000. Effect of processing conditions on crystallization kinetics of a milk fat model system. Journal of the American Oil Chemists' Society 77(11): 1177-1187.

Herrera, M.L. and Hartel, R.W. 2000. Effect of processing conditions on physical properties of a milk fat model system. Journal of the American Oil Chemists' Society 77(11): 1197-1204.

Jacobsberg, B. and Jacqmain, D. 1976. Palm oil fractionation as related to the crystallization properties of triglycerides. Malaysian International Symposium on Palm Oil Processing and Marketing pp.1-23.

Kawamura, K. 1979. The DSC thermal analysis of crystallization behavior in palm oil. Journal of the American Oil Chemists' Society 56(8): 753-758.

Kawamura, K. 1980. The DSC thermal analysis of crystallization behavior in palm oil II. Journal of the American Oil Chemists' Society 57: 48-52.

Kellens, M. 1994. Developments in fat fractionation technology. Fats and oils and fats group symposium Fractional crystallization of fats. London 9 March.

Kougoulos, E., Jones, A.G. and Wood-Kaczmar, M.W. 2005. Estimation of crystallization kinetics for an organic fine chemical using a modified continuous coolig mixed suspension mixed product removal (MSMPR) crystallizer. Journal of Crystal Growth 273: 520-528.

Litwinenko, J.W., Rojas, A.M., Gerschenson, L.N. and Marangoni, A.G. 2001. The relationship between crystallization behaviour, microstructure and mechanical properties in a palm oil-based shortening. Proceedings of the 2001 PIPOC International Palm Oil Congress (Chemistry and Technology). Pp. 169-183.

Patience, D.B., Hartel, R.W. and Illingworth, D. 1999. Crystallization and pressure filtration of anhydrous milk fat: Mixing effects. Journal of the American Oil Chemist's Society 76(5): 585-594.

SAS Institute Inc. 1989. The SAS system for windows, SAS Institute NC, USA.

Taylor, A.M. 1976. The crystallization and dry fractionation of Malaysian palm oil. Oleagineux 31(2): 73-79.

Timms, R.E. 1994. Theory and kinetics of fractional crystallization of fats. Lecture papers from the Oil and Fats group symposium Fractional crystallization of fats, pp.1-9. London.

Timms, R.E. 2005. Fractional crystallization – the fat modification process for the 21st century. European Journal of Lipid Science and Technology 107:48-57.

van Putte, K.P.A.M. and Bakker, B.H. 1987. Crystallization kinetics of palm oil. Journal of the American Oil Chemist' Society 64 (8): 1138-1143.

Yu, Z.Q., Tan, R.B.H. and Chow, P.S. 2005. Effects of operating conditions on agglomeration and habit of paracetamol crystals in anti-solvent crystallization. Journal of Crystal Growth 279: 477-488.

Zauner, R. and Jones, A.G. 2000. Determination of nucleation, growth, agglomeration and disruption kinetics from experimental precipitation data: the calcium oxalate system. Chemical Engineering Science 55: 4219-4232.